J. exp. Biol. 151, 405–422 (1990)
Printed in Great Britain © The Company of Biologists Limited 1990

A QUANTITATIVE DESCRIPTION OF NODAL MEMBRANE CURRENTS IN MYELINATED NERVE FIBRES OF THE LIZARD *ANOLIS CAROLINENSIS*

BY EVELYNE BENOIT

Laboratoire de Physiologie comparée, U.R.A. C.N.R.S. 1121, bâtiment 443, Université Paris Sud, F-91405 Orsay, France

Accepted 16 March 1990

Summary

Experiments were performed on individual nodes of Ranvier from a lizard at 15–16°C, using the method of Nonner (1969). In addition to a leakage current (mean conductance of 19.7 nS), the membrane ionic currents consisted of a Na^+ current, completely inhibited by 1 μmol l^{-1} external tetrodotoxin, and a K^+ current, sensitive to external tetraethylammonium ions and to internal caesium ions. The inactivation time course of the Na^+ current at 0 mV was well fitted by the sum of two exponential phases, one fast and one slow, with mean time constants of 0.68 and 2.92 ms, respectively. In contrast to observations on amphibian and mammalian preparations, the peak Na^+ current showed an almost linear potential dependence at large positive membrane potentials. A mean maximum Na^+ conductance of 146.8 nS was calculated. Both the time and potential dependence of the K^+ current indicated that it was similar to that found in amphibian nodes of Ranvier. The mean maximum K^+ conductance was 51.9 nS. Furthermore, as described in amphibians, three different components of the K^+ current (s, f_1 and f_2) could be separated. We conclude that, under similar experimental conditions, nodal ionic currents are qualitatively and quantitatively similar in lizard and amphibian myelinated nerve fibres, suggesting that the nodal membrane of these two preparations contains similar types of ionic channels. These results strengthen the view that the near absence of nodal K^+ channels is a peculiarity of mammalian nerves.

Introduction

Our knowledge of ionic channels associated with saltatory conduction in myelinated nerve fibres is largely based on experiments on amphibians, which have often served as models for the nervous system of mammals. Although the ionic basis of nerve excitation was first elucidated in the squid giant axon (Hodgkin and Huxley, 1952), later experiments on amphibian nodes of Ranvier revealed a similar mechanism for action potential generation: an early transient increase in permeability to Na^+ which underlies the depolarization of the nerve membrane,

Key words: lizard axons, nodes of Ranvier, Na^+ and K^+ channels.

and a delayed increase in permeability to K^+ which is largely responsible for the membrane repolarization (Dodge and Frankenhaeuser, 1958).

Studies on mammalian nodes of Ranvier have found that the delayed outward K^+ current is either very small or virtually absent, and that the leakage current provides the main part of the repolarizing outward current. In contrast, there are many similarities in the early transient Na^+ current of amphibian and mammalian myelinated nerve fibres (Chiu *et al.* 1979; Brismar, 1980; Brismar and Schwarz, 1985). Thus, it appears that the main difference between the amphibian and mammalian nodal membrane is that, in the latter, K^+ channels are either greatly reduced in number or absent.

Little information is available on the pattern of ionic channel distribution in other vertebrate peripheral nerves. We therefore examined the nodal membrane currents in myelinated nerve fibres of a reptile, where recent studies have shown that tetraethylammonium ions (TEA^+) prolong the intra-axonally recorded action potential, suggesting that the nodal membrane contains substantial K^+ currents (Barrett *et al.* 1988).

A preliminary account of part of this work has appeared elsewhere (Angaut-Petit *et al.* 1989).

Materials and methods

The experiments were carried out on nodes of Ranvier of isolated myelinated nerve fibres from the sciatic nerve of the lizard *Anolis carolinensis* (Daudin). Prior to dissection, the lizard was anaesthetized by cold and then its head was removed with a single cut.

The membrane potential and membrane currents were recorded under current- and voltage-clamp conditions, using the method of Nonner (1969). The node under investigation was stimulated at a frequency of 0.7 Hz. As previously described in amphibian and mammalian myelinated nerve fibres (Stämpfli and Hille, 1976; Brismar, 1980; Neumcke and Stämpfli, 1982), the holding potential was adjusted to give a 30 % inactivation of the peak transient (Na^+) current recorded at 0 mV, and thus corresponded to the normal resting potential. In the present experiments, the resting potential of the fibres was not measured. However, previous studies on intra-axonally recorded action potentials reported that the measured resting potential of lizard fibres was in the range -50 to -85 mV (Barrett and Barrett, 1982; Barrett *et al.* 1988). Therefore, we arbitrarily assumed that the normal resting potential, and thus the holding potential, was -70 mV. If not stated otherwise, under voltage-clamp the membrane was held at this level. Membrane currents were calculated assuming an axoplasmic resistance of 30 MΩ (see Barrett and Barrett, 1982). The series resistance was not compensated for.

All values are expressed as the mean±standard error of the mean of N different fibres. The linear regression analyses, the non-linear least-squares fits and the curves calculated from an equation were determined by computer. Some curves were drawn by eye.

The node was superfused with control Ringer's solution or test solutions. The Ringer's solution (pH 7.4) had the following composition (in mmol l^{-1}): NaCl, 111.5; KCl, 2.5; $CaCl_2$, 1.8; $NaHCO_3$, 2.4. In isotonic KCl solution, the NaCl was omitted and KCl was increased to 117 mmol l^{-1}. If not stated otherwise, the nerve fibre ends were cut in a solution containing 120 mmol l^{-1} KCl, which also bathed the ends of the fibres throughout the experiments. The temperature was maintained at 15–16°C.

Results

Membrane potential

The excitability of the isolated myelinated nerve fibre was tested under control conditions. Fig. 1A shows an action potential of about 80 mV peak amplitude and a threshold of about 30 mV, which was evoked by a brief (0.5 ms) suprathreshold depolarizing pulse of current. The threshold was determined as the difference between membrane potential and resting potential, corresponding to a liminal stimulation. In a sample of five fibres, the peak amplitude of action potentials ranged from 50 to 80 mV (mean 57.6±5.6 mV) and the threshold varied between 15 and 30 mV (mean 23.5±2.9 mV). The resting potential of the fibres was assumed to be in the range −50 to −85 mV (see Materials and methods) and thus

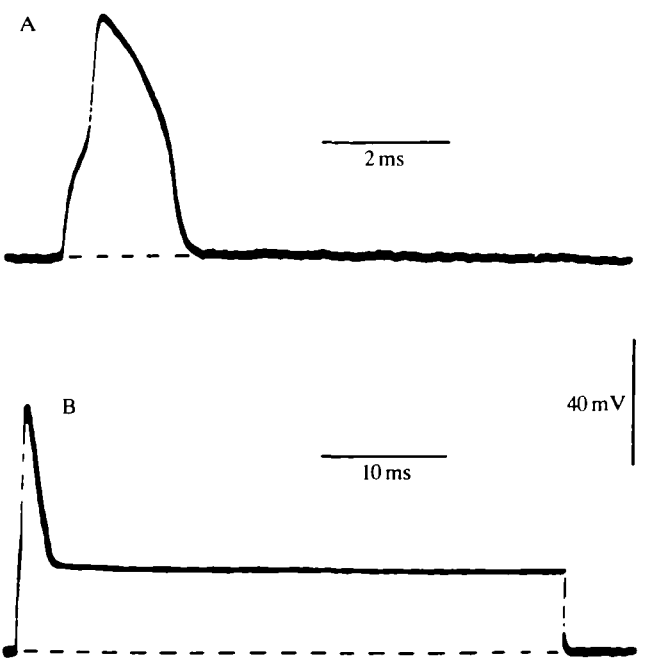

Fig. 1. Action potential of lizard myelinated nerve fibre. The action potentials were recorded in Ringer's solution with the cut ends of the axon in 120 mmol l^{-1} KCl and were elicited by suprathreshold depolarizing pulses of current of 0.5 ms (A) or 45 ms (B) duration. Dashed lines indicate the resting potential of the fibre.

these peak action potential amplitudes showed little or no overshoot. It must be noted that, considering the mean and S.E.M. of the peak amplitude of action potentials (see above), the action potential shown in Fig. 1A should be observed in less than 5 % of the preparations. The time course of the repolarization phase and the duration of action potentials were practically identical in all the fibres studied. The action potential duration, measured at half peak amplitude, was 1.6±0.2 ms (five fibres).

Long-lasting (35–45 ms) suprathreshold depolarizing pulses of current evoked only single action potentials and repetitive responses could not be elicited in any of the fibres tested (Fig. 1B).

If one assumes that the electrophysiological properties that characterize motor and sensory nerve fibres are identical in amphibian and lizard preparations, the present results strongly suggest that all the lizard fibres tested can be identified as motor fibres (Neumcke, 1981; Schwarz *et al.* 1983). Furthermore, the first phase of repolarization of action potentials (Fig. 1A) resembled that observed in motor, rather than sensory, nerve fibres of amphibian preparations (see Neumcke, 1981). It should be noted that similar results were obtained when fibre ends were either not cut or cut in a solution containing 112 mmol l^{-1} CsCl and 12 mmol l^{-1} NaCl (not shown).

Membrane currents

Membrane currents were recorded with voltage-clamp under control conditions (Fig. 2A). It can clearly be seen that the nodal ionic currents consisted of three components which can be identified kinetically as a time-independent current, an early transient current and a delayed current. In addition, these components showed different voltage sensitivities.

Time-independent current

During voltage steps to between −170 and −60 mV, in addition to the capacitative current, only a small time-independent current was detected (Fig. 2A, left traces). The conductance of the time-independent current was calculated from the slope of the current–voltage curve, which was linear between −170 and −60 mV (Fig. 2B), according to the equation:

$$g = I/(V - V_{eq}), \tag{1}$$

where g is the conductance, I is the current amplitude, V is the membrane potential and V_{eq} is the ionic equilibrium potential. In the present case, V_{eq} was the potential at which the current was zero (−70 mV). The slope of the current–voltage relationship was determined by a linear regression analysis of data points ($r^2 \geq 0.994$). The conductance was 19.7±1.7 nS (six fibres). In four fibres, neither the potential at which the current was zero nor the conductance were significantly affected by the addition of 1 μmol l^{-1} tetrodotoxin (TTX) or 1–20 mmol l^{-1} TEA^+ to the solution which bathed the fibres (Fig. 2B). Under the latter conditions, the delayed current, which was activated at potentials more

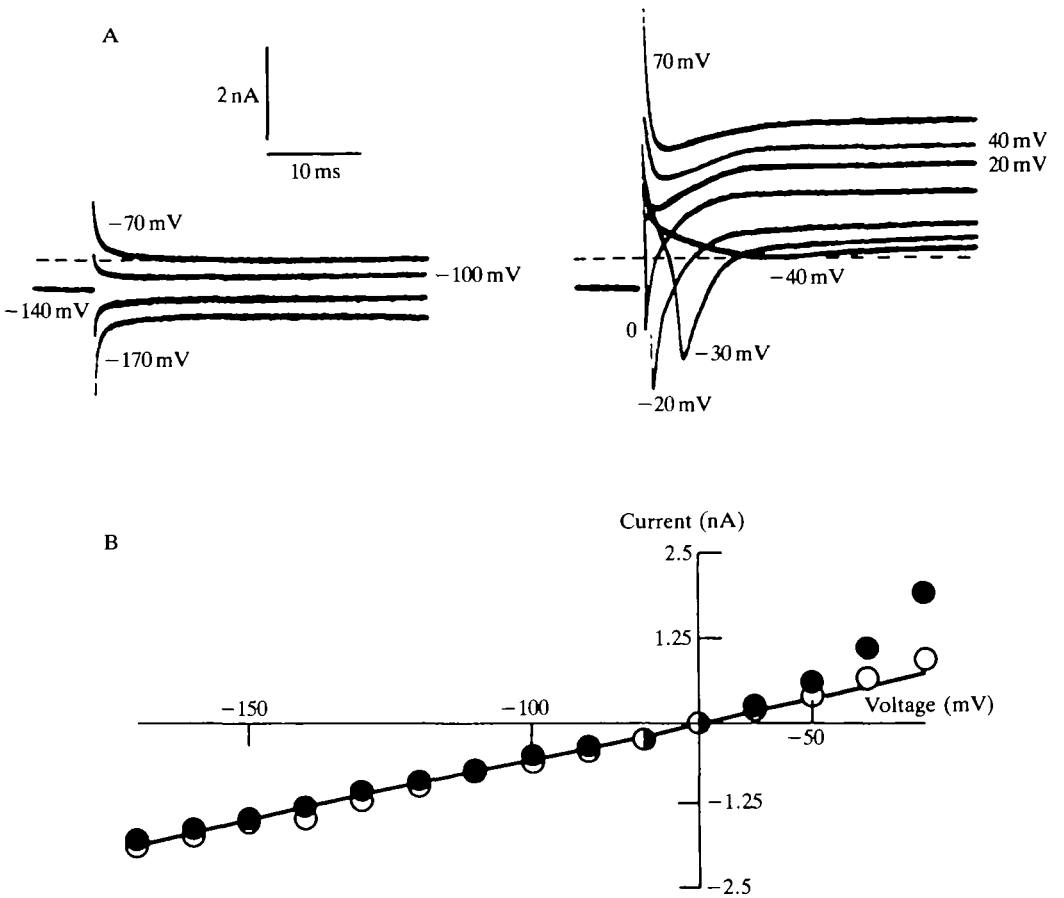

Fig. 2. Traces of membrane currents (A) and current–voltage relationships for the time-independent current (B) of lizard myelinated nerve fibre. The membrane currents were recorded during 35 ms pulses of various amplitudes preceded by a 50 ms hyperpolarization to −120 mV. (A) Family of current records obtained in Ringer's solution with the internal solution containing 120 mmol l^{-1} KCl. Dashed lines indicate the zero current level (at −70 mV). (B) Current–voltage relationships for the time-independent current measured at the end of pulses, before (filled circles) and after (open circles) addition of 1 μmol l^{-1} TTX and 20 mmol l^{-1} TEA^+ to the external solution. The straight line was drawn by eye. The conductances in this experiment, calculated according to equation 1 and determined by a linear regression analysis of data points ($r^2 \geq 0.997$), were 18.3 nS (filled circles) and 19.6 nS (open circles).

positive than −60 mV, was reduced (see also Fig. 7). It should be noted that, in two fibres, the conductance was not significantly modified when 112 mmol l^{-1} CsCl and 12 mmol l^{-1} NaCl were substituted for 120 mmol l^{-1} KCl in the solution bathing the cut ends of the axon.

This type of current clearly resembles the leakage current, which is a non-specific current, seen notably in squid, amphibian and mammalian nerves (Hodgkin and Huxley, 1952; Dodge and Frankenhaeuser, 1958; Chiu *et al.* 1979;

Brismar, 1980). In the remaining experiments, this current, with the capacitative current, was electronically subtracted off-line from the total current. For this purpose, the two currents were measured from the current associated with a 19–50 ms hyperpolarization to −140 mV, assuming a linear potential dependence.

Early transient current

An early inward or outward transient current could be detected both before (Fig. 2A, right traces) and after (inset of Fig. 3) subtraction of capacitative and

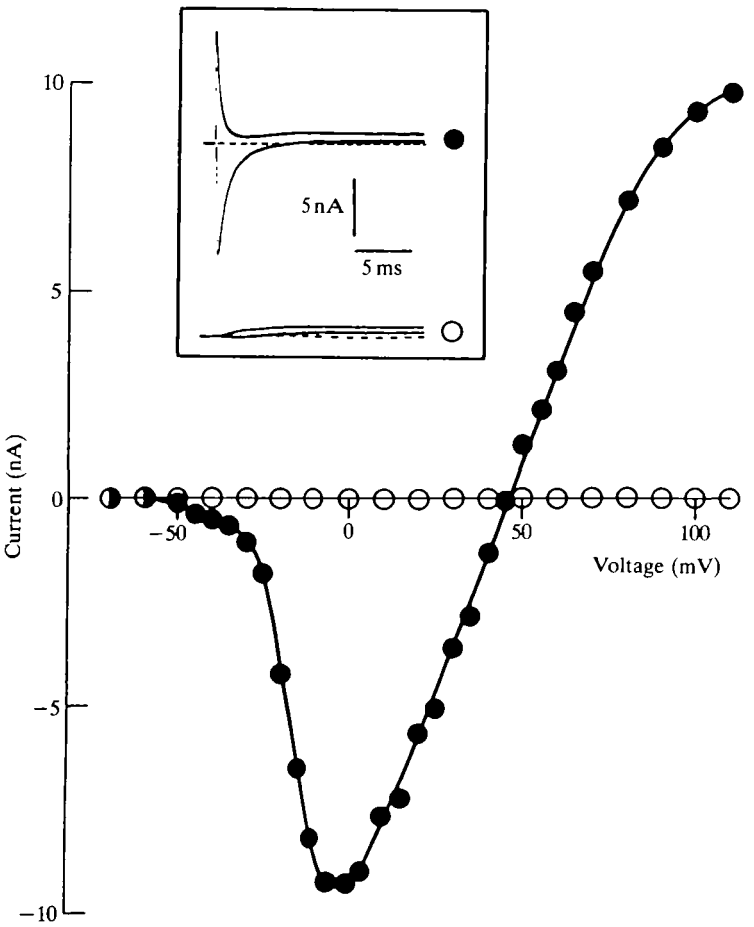

Fig. 3. Current–voltage relationships for the early transient current and the effect of TTX. The current was recorded during 19 ms depolarizing pulses of various amplitudes preceded by a 50 ms hyperpolarization to −120 mV, before (filled circles) and after (open circles) addition of 1 μmol l^{-1} TTX to the Ringer's solution which contained 20 mmol l^{-1} TEA^+. Internal solution: 120 mmol l^{-1} KCl. Capacitative and leakage currents have been subtracted. The peak amplitude of the early transient current was measured and plotted against membrane potential. The curve was drawn by eye. Inset: traces of currents recorded at 0 and 100 mV. Dashed lines indicate the zero current level.

leakage currents from the total current and addition of 20 mmol l^{-1} TEA^+ to the external solution. It should be noted that, in the presence of TEA^+, the delayed current was not completely suppressed (inset of Fig. 3, see also Fig. 7). The time course of activation of the early transient current, which was estimated from the time to peak, decreased with increasing depolarizations and was 0.39±0.03 ms and 0.32±0.02 ms at −10 and 0 mV, respectively (11 fibres). To characterize the early transient current, the peak current–voltage relationship was plotted (Fig. 3). In 11 fibres, the current activated at −50.0±1.5 mV, the maximum peak inward current was −7.57±0.98 nA at a membrane potential of −13±2 mV, and the reversal potential was 46.4±4.0 mV. In four fibres, the substitution of 112 mmol l^{-1} CsCl and 12 mmol l^{-1} NaCl for 120 mmol l^{-1} KCl in the solution bathing the cut ends of fibres did not significantly modify these values. In particular, in the latter experiments, the reversal potential for the current was 41.8±9.1 mV. The addition of 1 μmol l^{-1} TTX to the external solution completely inhibited the early transient current (Fig. 3).

This early transient current clearly exhibited the characteristics of the voltage-gated sodium current present in excitable membranes and, in particular, in amphibian and mammalian nodes of Ranvier (Dodge and Frankenhaeuser, 1959; Chiu *et al.* 1979; Brismar, 1980). However, in contrast to what has been reported in other preparations, the current–voltage curve in the lizard showed little if any rectification and was almost linear at large depolarizations (Fig. 3), whether the solution bathing the cut ends of fibres was 120 mmol l^{-1} KCl or 112 mmol l^{-1} CsCl and 12 mmol l^{-1} NaCl. Thus, to describe the activation state of the Na^+ system, the Na^+ conductance was calculated from the current–voltage curve according to equation 1 where V_{eq} was the reversal potential for the Na^+ current. The maximum Na^+ conductance was 146.8±20.7 nS (11 fibres).

The potential dependence of the inactivation process was investigated with the classical two-pulse protocol, and is presented in Fig. 4. The steepness factor of the curve was 8.9 mV and the membrane potential corresponding to half-maximum steady-state inactivation was −56.4 mV. It should be noted that, for membrane potentials more negative than −150 mV, the peak Na^+ current decreased and thus the steady-state Na^+ inactivation increased. This may result from a slowing down of the turning-on of the Na^+ current induced by large prehyperpolarizations (see Chiu, 1977, Fig. 12) or may reflect a block by calcium ions (Dubois and Bergman, 1971; Rack and Drews, 1989). The time dependence of the inactivation process was studied by analysing the inactivation kinetics of the TTX-sensitive current, i.e. the current calculated as the difference between current traces recorded under control conditions and in the presence of 1 μmol l^{-1} TTX. Fig. 5 shows that, whereas at −40 mV the current declined in only one exponential phase, the time course of inactivation at 0 mV was better described by the sum of two exponentials, one fast and one slow. In six fibres, the inactivation time constants at 0 mV were 2.92±0.24 ms and 0.68±0.09 ms for the slow and fast phases, respectively, and the extrapolated value to time zero of the slow phase, relative to the sum of that of the slow and fast phases, was 18±5 %.

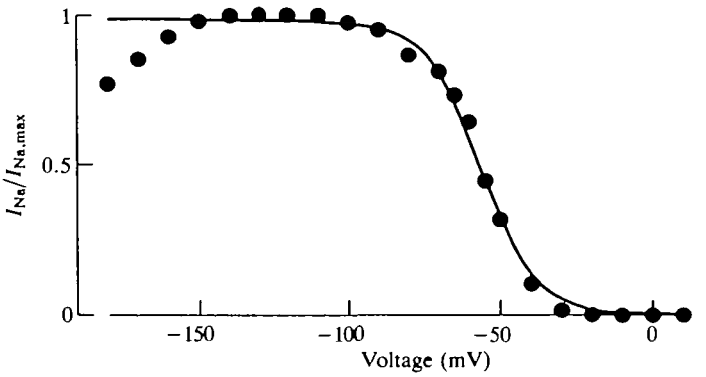

Fig. 4. Steady-state Na^+ inactivation–voltage relationship. The current was recorded in Ringer's solution with 20 mmol l^{-1} TEA^+, the internal solution containing 120 mmol l^{-1} KCl, during 35 ms depolarizing pulses to 0 mV preceded by 50 ms pulses of various amplitudes. The points are the values of the peak Na^+ current (I_{Na}), normalized to its maximum value ($I_{Na,max}$) at large negative voltages (from −100 to −140 mV). The curve was calculated from the equation:

$$I_{Na}/I_{Na,max} = 1/[1+\exp(V-\bar{V})/k],$$

where V is the membrane potential, $\bar{V}$ is the membrane potential for $I_{Na}/I_{Na,max}=0.5$ and k is the steepness factor. The values of the parameters $\bar{V}$ and k, determined by a non-linear least-squares fit of data points (from −150 to 10 mV), were −56.4 mV and 8.9 mV, respectively ($r^2=0.970$).

The values extrapolated to time zero and the time constants of the fast and slow components of Na^+ current inactivation, determined as described in Fig. 5, were plotted against membrane potential (Fig. 6). One point needs to be emphasized. Only one phase of inactivation was observed at −40 mV (see Fig. 5A). Does this phase correspond to either the fast, the slow or both the fast and slow components? In amphibian nodes of Ranvier, similar results were obtained and the authors concluded that the current near −40 mV was exclusively a slow component (Benoit *et al.* 1985). However, the extrapolation of the fast time constant–voltage curve to −40 mV gave a value close to that of the slow time constant, i.e. about 8 ms (Fig. 6), suggesting that both fast and slow components may exist at this potential. Under these conditions, it was not possible to determine the values extrapolated to time zero of the fast and slow components. It should be noted that similar results were obtained at −50 mV, although the time constant could not be accurately calculated.

Delayed current

In the presence of 1 μmol l^{-1} TTX and after subtraction of capacitative and leakage currents from the total current, a delayed outward current could be observed (inset of Fig. 7). The activation kinetics of this current, which was estimated from the time corresponding to half-maximum current amplitude, decreased with increasing depolarization and was 1.68±0.29 ms at 50 mV (eight

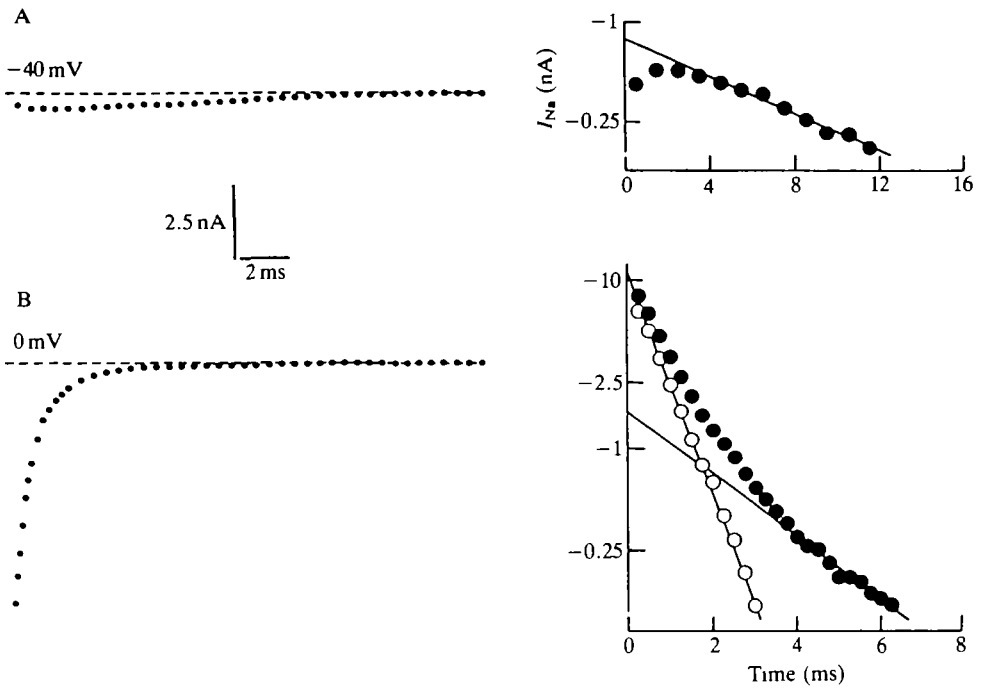

Fig. 5. Time dependence of Na^+ current inactivation. The current was recorded in Ringer's solution before and after addition of 1 μmol l^{-1} TTX, during 19 ms depolarizing pulses to −40 mV (A) and 0 mV (B) preceded by a 50 ms hyperpolarization to −120 mV. Internal solution: 120 mmol l^{-1} KCl. Representations in normal (left panels) and semilogarithmic (right panels) coordinates of the inactivation kinetics of the Na^+ current calculated as the difference between current traces recorded without and with TTX. In the left panels, dashed lines indicate the zero current level. In the right panels, filled circles (A and B) represent the total TTX-sensitive current and open circles (B) represent the fast phase of inactivation after subtraction of the slow phase of inactivation (straight line through filled circles). The values extrapolated to time zero and the time constants of inactivation components were determined by linear regression analyses ($r^2 \geq 0.970$) using logarithms of the measured values. In A, the initial amplitude and the time constant of the component were −0.77 nA and 7.77 ms, respectively. In B, the initial amplitudes and the time constants were, respectively, −1.65 nA and 2.37 ms (slow component) and −10.66 nA and 0.68 ms (fast component).

fibres). The current–voltage relationship for the delayed current is shown in Fig. 7. In eight fibres, the activation potential of the delayed current, defined as the membrane potential corresponding to about 1% of maximum delayed conductance, was −52.9±1.6 mV. Addition of 20 mmol l^{-1} TEA^+ to the external solution greatly inhibited the K^+ current (Fig. 7).

These results indicated that the delayed current was a potassium current similar to that previously found in squid (Hodgkin and Huxley, 1952), in amphibian (Frankenhaeuser, 1962*a*) and, although much smaller, in mammalian (Brismar and Schwarz, 1985) nerves. The maximum K^+ conductance was determined from

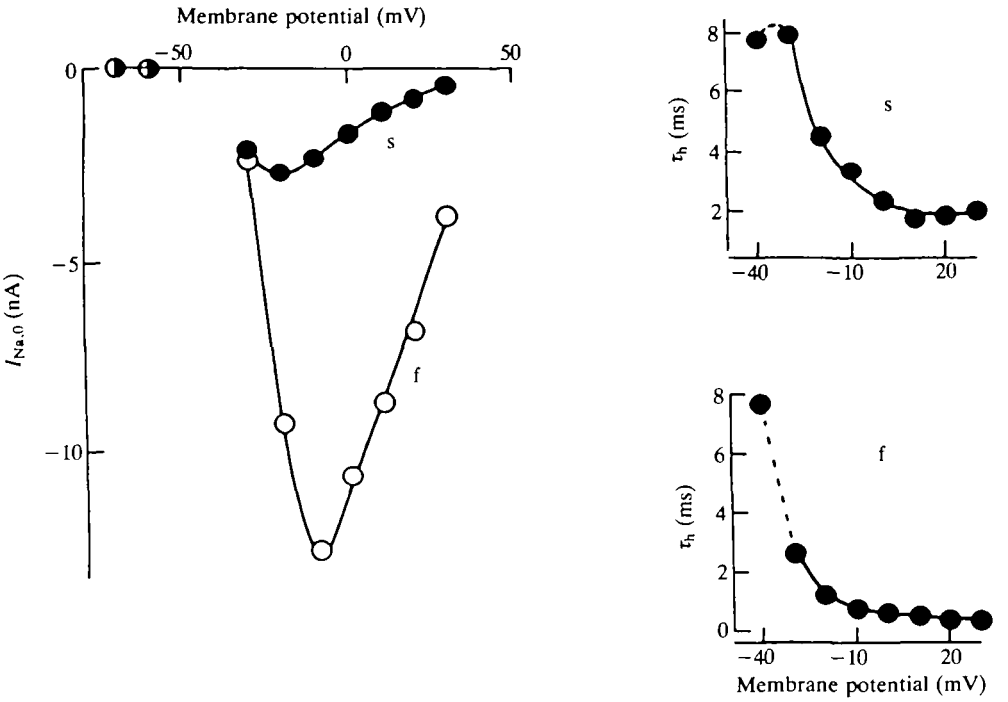

Fig. 6. Potential dependence of the fast and slow components of Na^+ current inactivation. The TTX-sensitive current was calculated during 19 ms depolarizing pulses of various amplitudes preceded by a 50 ms hyperpolarization to −120 mV and, for each pulse, the inactivation time course of the current was separated into fast (f) and slow (s) phases, as described in Fig. 5. The values extrapolated to time zero, $I_{Na,0}$ (left panel: filled circles for s and open circles for f) and the time constants, τ_h (right panels: upper for s and lower for f) of the two components were determined by linear regression analyses ($r^2 \geq 0.970$) using logarithms of the measured values, and plotted against membrane potential (mV). Curves were drawn by eye.

the current–voltage curve, according to equation 1, where V_{eq} was the equilibrium potential of K^+, i.e. −96.3 mV calculated from the Nernst equation, and was 51.9±15.7 nS (eight fibres).

Substitution of Cs^+ for K^+ in the 'internal solution' that bathed the cut ends of the fibres also contributed to an inhibition of the K^+ current (Fig. 8A). In contrast to the effect of external TEA^+, the blockage induced by internal Cs^+ was dependent on the membrane potential (Fig. 8B). Between −40 and 100 mV, the relative K^+ current in the presence of TEA^+ was constant and equalled 0.33±0.01, whereas that in the presence of Cs^+ first decreased from 0.58 at −40 mV to 0.27 at 20 mV and then remained constant at 0.26±0.01 from 20 to 100 mV. It should be noted that, in the presence of internal Cs^+, the remaining K^+ current recorded at 30 mV was further reduced to 0.07±0.01 by external application of 20 mmol l^{-1} TEA^+ (three fibres), relative to that recorded under control conditions.

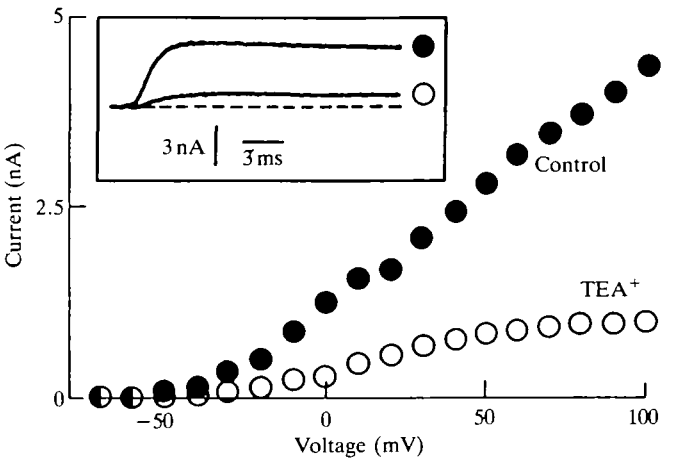

Fig. 7. Current–voltage relationships for the delayed current and the effect of external TEA^+. The delayed current was recorded during 19 ms depolarizing pulses of various amplitudes, before (filled circles) and after (open circles) addition of 20 mmol l^{-1} TEA^+ to the Ringer's solution which contained 1 μmol l^{-1} TTX. Internal solution: 120 mmol l^{-1} KCl. Capacitative and leakage currents have been subtracted. The amplitude of the delayed current was measured at the end of the pulses and plotted against membrane potential. Inset: traces of currents recorded at 100 mV. Dashed line indicates the zero current level.

In amphibian nodes of Ranvier, three different K^+ currents have been characterized and separated (Dubois, 1981, 1983; Benoit and Dubois, 1986; Plant, 1986). In that preparation, when recorded in an isotonic KCl solution, the tail of the K^+ current following repolarization decreased in two phases: a fast one and a slow exponential one. To determine whether such phases also exist in lizard nodes of Ranvier, K^+ tail currents were recorded. The K^+ current, activated by the conditioning depolarizing pulses, deactivated upon repolarization in several phases (Fig. 9A). Whereas after a depolarizing pulse to −80 mV only a single slow exponential phase(s) could be detected, the K^+ tail current recorded after −60 or +20 mV decreased in two phases, a slow one (s) and a fast one (f), as previously described in amphibian nodes of Ranvier (see above). The time constants of the slow and fast phases were, respectively, 26.5 and 5 ms (−60 mV) and 57.5 and 11 ms (20 mV). The slow and fast K^+ conductances were determined from the instantaneous slow component (obtained by exponentially extrapolating, on a semilogarithmic scale, the later part of the tail current to time zero of repolarization) and the fast component (total tail current minus instantaneous slow component), respectively, according to equation 1, where V_{eq} was the equilibrium potential of K^+, i.e. −0.6 mV calculated from the Nernst equation. Fig. 9B shows conductance–voltage curves for the slow and fast components of the K^+ tail current, corresponding to a representative experiment. The fast component activated at more positive membrane potentials than the slow component. In addition, whereas the slow conductance(s) increased almost monotonically with

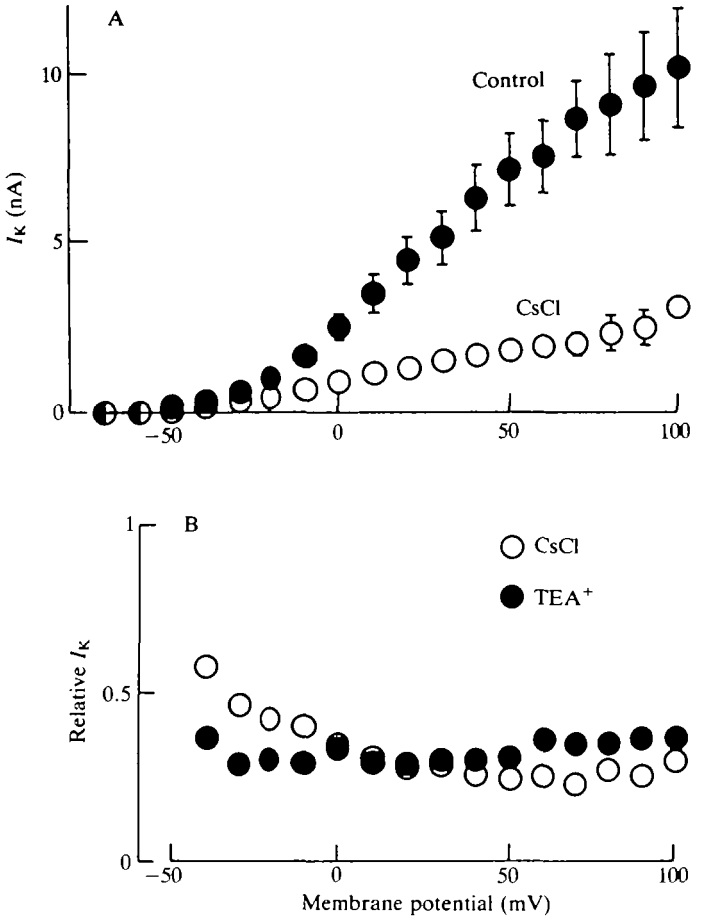

Fig. 8. Action of Cs^+ and the potential dependence of the effects of Cs^+ and TEA^+ on the K^+ current. (A) The amplitude of the K^+ current was measured at the end of 19–50 ms depolarizing pulses of various amplitudes in Ringer's solution containing 1 μmol l^{-1} TTX. The solution bathing the cut ends of the axons was either 120 mmol l^{-1} KCl (filled circles) or 112 mmol l^{-1} CsCl and 12 mmol l^{-1} NaCl (open circles). In each case, the results obtained from four fibres have been plotted against membrane potential. (B) Ratio of mean values (four fibres in each case) of K^+ current amplitude measured in the presence of either 112 mmol l^{-1} internal Cs^+ (open circles), as described above, or 20 mmol l^{-1} external TEA^+ (filled circles), as described in Fig. 7, and under control conditions, i.e. external Ringer's solution with 1 μmol l^{-1} TTX and internal 120 mmol l^{-1} KCl solution, *vs* membrane potential.

more positive membrane potentials and then reached a constant value, the conductance–voltage curve for the fast component showed a marked bend between −40 and 0 mV. According to Dubois (1981), one explanation for this curve is that it consists of the sum of two superimposed conductance–voltage curves corresponding to two K^+ components: one (f_1) activating between −80 and

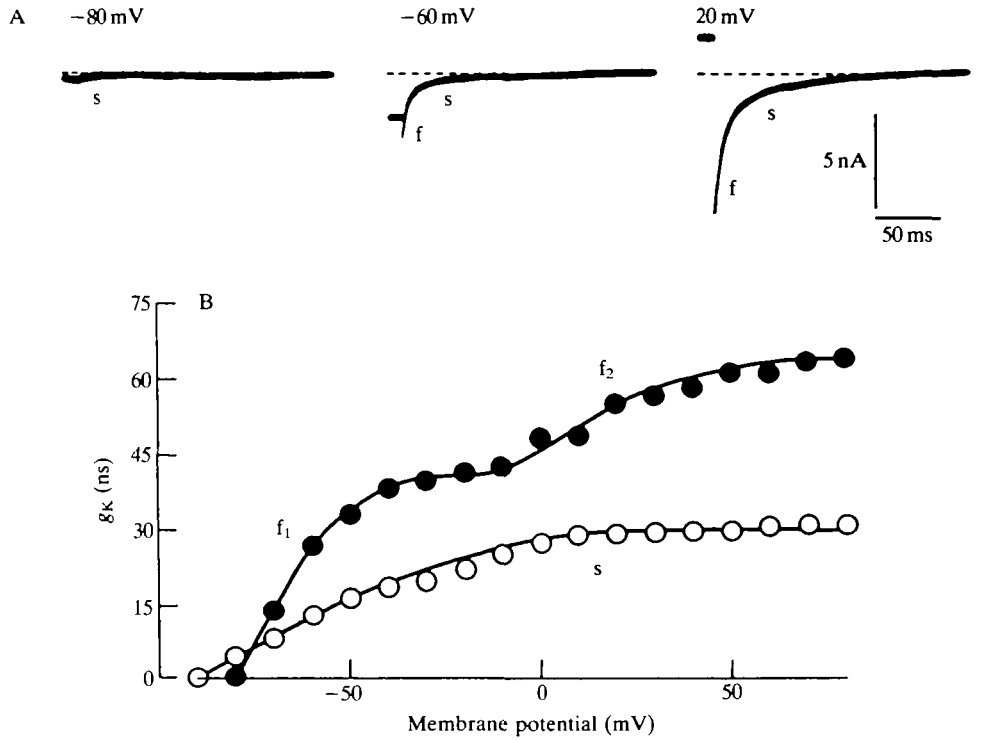

Fig. 9. Three different components of the K^+ current. The K^+ tail current was recorded upon repolarization to a holding potential of −90 mV, following 100 ms conditioning depolarizing pulses of various amplitudes, in an isotonic KCl solution containing 1 μmol l^{-1} TTX. Internal solution: 120 mmol l^{-1} KCl. (A) K^+ tail current traces recorded after depolarizing pulses to −80, −60 and +20 mV. Capacitative and leakage currents have been subtracted. Dashed lines indicate the zero current level (without depolarizing pulse). (B) Conductance–voltage relationships for slow (open circles) and fast (filled circles) phases of the K^+ tail current. Slow and fast conductances were calculated as described in the text and plotted against membrane potential during conditioning depolarizing pulses. The curves were drawn by eye.

−20 mV, and another (f_2) activating between −10 and +70 mV. The relative values for s, f_1 and f_2 maximum conductances were 32, 43 and 25 %, respectively.

Discussion

This paper reports results obtained from a detailed voltage-clamp investigation of lizard myelinated nerve fibres. The results show that the nodal ionic currents consist of three components which have been identified as a leakage current, an early transient Na^+ current and a delayed K^+ current. Each of these currents was similar to those previously described in amphibian nodes of Ranvier (see below).

Leakage current

The leakage current of the lizard nodal membrane is time-independent, has a

linear potential dependence and is zero at the holding potential (Fig. 2). The current is also not noticeably affected by specific blocking agents like TTX and TEA^+. These are also the characteristics of the leakage current in squid (Chang, 1986), rabbit (Chiu *et al.* 1979), rat (Brismar, 1980; Brismar and Schwarz, 1985) and frog (Hille, 1967, 1973; Dubois and Bergman, 1975).

Early transient Na^+ current

The early transient Na^+ current is clearly similar to that present in most excitable membranes. First, it is completely inhibited by 1 μmol l^{-1} TTX (Fig. 3). Second, it exhibits a reversal potential close to, although slightly more negative than, the expected Nernstian potential for Na^+. When the solution bathing the cut ends of fibres contained either 120 mmol l^{-1} KCl or 112 mmol l^{-1} CsCl and 12 mmol l^{-1} NaCl, the mean reversal potentials for the Na^+ current were 46.4 and 41.8 mV, respectively (Fig. 3). Assuming that the internal concentration of Na^+ is identical to that of the external compartments in which the cut ends of the fibres were bathed, an equilibrium potential for Na^+ of 55.9 mV can be calculated from the Nernst equation, using external and internal concentrations of Na^+ of 113.9 and 12 mmol l^{-1}, respectively. To account for this discrepancy, one explanation could be that the channels associated with the Na^+ current are only selective for Na^+, but that the effective axoplasmic concentration of Na^+ is more than 12 mmol l^{-1}. In contrast, another explanation is that the effective axoplasmic concentration of Na^+ is 12 mmol l^{-1}, but that the Na^+ current is not exclusively carried by Na^+ but also, although to a lesser extent, by other ions such as K^+ and Cs^+. That the Na^+ current–voltage curve in the lizard is almost linear at large depolarizations supports the latter explanation, since the rectification shown by the curve in amphibian and mammalian nodes of Ranvier has been attributed to the rectification which appears in a permeable membrane with different concentrations of current-carrying ions on either side (see Dodge and Frankenhaeuser, 1959; Brismar, 1980). Our results may thus suggest that the ionic selectivity of Na^+ channels for Na^+ is less in lizard than in amphibian and mammalian nerves. Further experiments are needed to establish this point.

The lizard Na^+ current has a potential-dependent inactivation curve (Fig. 4) with a shape similar to that for the Na^+ current in amphibian and mammalian nodes of Ranvier. Because the holding potential is usually set to give a steady-state Na^+ inactivation of a definite value (see Materials and methods), an eventual shift along the potential axis of the steady-state Na^+ inactivation–voltage curve cannot be detected. Nevertheless, the slope of the curve, as defined by the steepness factor, does not vary significantly among the different preparations (Frankenhaeuser, 1959; Chiu *et al.* 1979).

Under similar experimental conditions, the kinetics of Na^+ current inactivation have been reported to be 2–3 times faster in amphibian than in mammalian nodal membrane (Chiu *et al.* 1979). Nevertheless, in both preparations, it has been described as a second-order process (Chiu, 1977; Neumcke and Stämpfli, 1982). In the present work (Figs 5 and 6), the inactivation time course of the Na^+ current is

well fitted by the sum of two exponential phases with time constants and potential dependence similar to those in amphibian nodes of Ranvier (Schwarz *et al.* 1983; Benoit *et al.* 1985; Benoit and Dubois, 1987). However, further experiments are needed to determine whether these two phases result from the existence of several inactivated or several open states of Na^+ channels, or if they correspond to two distinct Na^+ currents flowing through two different types of Na^+ channels (see Benoit *et al.* 1985).

Delayed K^+ current

The time course and potential dependence of the substantial delayed K^+ current (Figs 7 and 8A) clearly exhibit the characteristics of the K^+ current in squid axon and amphibian nodes of Ranvier (Hodgkin and Huxley, 1952; Frankenhaeuser, 1962*a*). Furthermore, the three different components of the K^+ current in the lizard (Fig. 9) are almost identical to those described in amphibians (Dubois, 1981), which suggests that at least three types of K^+ channels may also exist in the lizard nodal membrane. It should be noted that a comparison with mammalian nerves is not possible since, in the rabbit, the nodal K^+ current is virtually absent (Chiu *et al.* 1979), whereas in the rat, only a small nodal delayed K^+ current has been identified (Brismar, 1980; Brismar and Schwarz, 1985). Nevertheless, the existence of at least two distinct types of K^+ channels has been recently suggested in the latter preparation (Röper and Schwarz, 1989).

External TEA^+ blocks the lizard K^+ current, the blockage being independent of the membrane potential (Figs 7 and 8B). The effect of TEA^+ is similar to that in amphibians except that TEA^+ is more effective in the latter case (Hille, 1967). In the squid axon, TEA^+ was only effective from the inside (Armstrong, 1966). In rat nodes of Ranvier, it can be calculated that the K^+ current remaining after external application of 20 mmol l^{-1} TEA^+ is about 30 % of its control value (Brismar and Schwarz, 1985). This suggests that the K^+ current is as sensitive to TEA^+ in the lizard as it is in the rat. However, in the latter preparation, a much higher degree of blockage than that previously reported (see above) has been recently shown (Röper and Schwarz, 1989).

Finally, as in squid and amphibian axons (see Dubois, 1983), the lizard K^+ current is much reduced when Cs^+ is present in the axoplasm, the outward current being increasingly blocked by internal Cs^+ as the membrane potential is made increasingly positive (Fig. 8). However, the inhibition is incomplete, even at high positive membrane potentials, leaving a small residual outward current. If one assumes that Cs^+ diffuses through the axoplasm and reaches the nodal membrane, such an outward current may be mainly carried by Cs^+ passing through K^+ channels (see Clay and Shlesinger, 1984). That the 'Cs^+-insensitive outward current' is reduced by TEA^+ supports this interpretation.

Concluding remarks

In this study of the activation state of lizard Na^+ and K^+ systems, the observation of an almost linear Na^+ current–voltage curve (Fig. 3) induced us to

use conductances rather than permeabilities calculated from the constant field equation (see Angaut-Petit *et al.* 1989). In addition, the existence of several components of both Na^+ and K^+ currents which have different potential sensitivities (Figs 6 and 9) and also K^+ accumulation in the nodal gap (see Dubois, 1983) complicate analysis with the constant field equation. Nevertheless, the ratio of maximum K^+ and Na^+ conductances is identical to that of maximum K^+ and Na^+ permeabilities (see Angaut-Petit *et al.* 1989); it is 0.35, a value close to that obtained in amphibian nodes of Ranvier (Frankenhaeuser, 1959, 1962*b*), but four- to sixfold higher than the value determined in rat myelinated nerve fibres (Brismar *et al.* 1987). Furthermore, when determined in an isotonic KCl solution, where the artefacts induced by K^+ accumulation are minimized (see Dubois, 1983), the contribution of the slow K^+ component to the total K^+ conductance is 32 % in the lizard (Fig. 9). This value is much nearer to that in amphibian nerves (about 20 %, Dubois, 1981, 1983) than to that in rat nerves (about 80 %, Röper and Schwarz, 1989).

The leakage conductance calculated in this study (19.7 nS), which accounts for only about 9 % of the total maximum conductance, agrees better with the earlier data of 15–18 nS for amphibians (Frankenhaeuser and Huxley, 1964; Brismar, 1982) than with that of 29–33 nS for mammals (Chiu *et al.* 1979; Brismar, 1980; Brismar and Schwarz, 1985). However, since these absolute values depend markedly on how the current calibration was made, a close comparison between the different species is difficult. In contrast, the ratio of leakage and maximum K^+ conductances ($g_L/g_{K,max}$), which indicates the relative roles played by leakage and K^+ currents in repolarizing the membrane, can be compared between the different types of axons. In this study, $g_L/g_{K,max}$ is 0.38. This value is about 50 times greater than the $g_L/g_{K,max}$ ratio in the squid (Hodgkin and Huxley, 1952) and at least 10 times lower than that in the rat (see Brismar, 1980), but is only twice as high as that in the frog (Hille, 1971). In the rabbit, the K^+ current has been reported to be lacking (Chiu *et al.* 1979). It thus appears that, whereas in the squid the K^+ current plays an important role in repolarizing the membrane, it plays a secondary role in the lizard, as in the frog, and is almost unnecessary in repolarizing the mammalian nodal membrane. This is in agreement with the effect of TEA^+ on the action potential duration, which varies among the different types of axons (Armstrong, 1966; Stämpfli and Hille, 1976; Brismar *et al.* 1987; Barrett *et al.* 1988).

Thus, under similar experimental conditions, lizard and amphibian myelinated nerve fibres exhibit qualitatively and quantitatively similar nodal ionic currents and thus identical excitability properties. In particular, the ionic mechanism of repolarization of the action potential is the same in the two preparations. The present results strengthen the view that the near absence of nodal K^+ current is a peculiarity of mammalian nerves.

I would like to thank J. M. Dubois for helpful comments on the manuscript and suggestions during the progress of this work. I am greatly indebted to I. Findlay for critical reading of the manuscript, and to D. Angaut-Petit and A. Mallart for

valuable discussions. This work was supported by a grant from INSERM (CRE 866006).

References

ANGAUT-PETIT, D., BENOIT, E. AND MALLART, A. (1989). Membrane currents in lizard motor nerve terminals and nodes of Ranvier. *Pflügers Arch. Eur. J. Physiol.* **415**, 81–87.

ARMSTRONG, C. M. (1966). Time course of TEA^+-induced anomalous rectification in squid giant axons. *J. gen. Physiol.* **50**, 491–503.

BARRETT, E. F. AND BARRETT, J. N. (1982). Intracellular recording from vertebrate myelinated axons: mechanism of the depolarizing afterpotential. *J. Physiol., Lond.* **323**, 117–144.

BARRETT, E. F., MORITA, K. AND SCAPPATICCI, K. A. (1988). Effects of tetraethylammonium on the depolarizing after-potential and passive properties of lizard myelinated axons. *J. Physiol., Lond.* **402**, 65–78.

BENOIT, E., CORBIER, A. AND DUBOIS, J. M. (1985). Evidence for two transient sodium currents in the frog node of Ranvier. *J. Physiol., Lond.* **361**, 339–360.

BENOIT, E. AND DUBOIS, J. M. (1986). Toxin I from the snake *Dendroaspis polylepis polylepis*: a highly specific blocker of one type of potassium channel in myelinated nerve fiber. *Brain Res.* **377**, 374–377.

BENOIT, E. AND DUBOIS, J. M. (1987). Interactions of guanidinium ions with sodium channels in frog myelinated nerve fibre. *J. Physiol., Lond.* **391**, 85–97.

BRISMAR, T. (1980). Potential clamp analysis of membrane currents in rat myelinated nerve fibres. *J. Physiol., Lond.* **298**, 171–184.

BRISMAR, T. (1982). Potassium permeability in thin amphibian myelinated fibres. *Pflügers Arch. Eur. J. Physiol.* **393**, 348–350.

BRISMAR, T., HILDEBRAND, C. AND BERGLUND, S. (1987). Voltage-clamp analysis of nodes of Ranvier in regenerated rat sciatic nerve. *Brain Res.* **409**, 227–235.

BRISMAR, T. AND SCHWARZ, J. R. (1985). Potassium permeability in rat myelinated nerve fibres. *Acta physiol. scand.* **124**, 141–148.

CHANG, D. C. (1986). Is the K permeability of the resting membrane controlled by the excitable K channel? *Biophys. J.* **50**, 1095–1100.

CHIU, S. Y. (1977). Inactivation of sodium channels: second order kinetics in myelinated nerve. *J. Physiol., Lond.* **273**, 573–596.

CHIU, S. Y., RITCHIE, J. M., ROGART, R. B. AND STAGG, D. (1979). A quantitative description of membrane currents in rabbit myelinated nerve. *J. Physiol., Lond.* **292**, 149–166.

CLAY, J. R. AND SHLESINGER, M. F. (1984). Analysis of the effects of cesium ions on potassium channel currents in biological membranes. *J. theor. Biol.* **107**, 189–201.

DODGE, F. A. AND FRANKENHAEUSER, B. (1958). Membrane currents in isolated frog nerve fibre under voltage clamp conditions. *J. Physiol., Lond.* **143**, 76–90.

DODGE, F. A. AND FRANKENHAEUSER, B. (1959). Sodium currents in the myelinated nerve fibre of *Xenopus laevis* investigated with the voltage clamp technique. *J. Physiol., Lond.* **148**, 188–200.

DUBOIS, J. M. (1981). Evidence for the existence of three types of potassium channels in the frog Ranvier node membrane. *J. Physiol., Lond.* **318**, 297–316.

DUBOIS, J. M. (1983). Potassium currents in the frog node of Ranvier. *Prog. Biophys. molec. Biol.* **42**, 1–20.

DUBOIS, J. M. AND BERGMAN, C. (1971). Conductance sodium de la membrane nodale: inhibition compétitive calcium–sodium. *C. R. hebd. Séanc. Acad. Sci. Paris* **272**, 2924–2927.

DUBOIS, J. M. AND BERGMAN, C. (1975). Late sodium current in the node of Ranvier. *Pflügers Arch. Eur. J. Physiol.* **357**, 145–148.

FRANKENHAEUSER, B. (1959). Steady-state inactivation of sodium permeability in myelinated nerve fibres of *Xenopus laevis*. *J. Physiol., Lond.* **148**, 671–676.

FRANKENHAEUSER, B. (1962*a*). Delayed currents in myelinated nerve fibres of *Xenopus laevis* investigated with voltage clamp technique. *J. Physiol., Lond.* **160**, 40–45.

FRANKENHAEUSER, B. (1962*b*). Potassium permeability in myelinated nerve fibres of *Xenopus laevis*. *J. Physiol., Lond.* **160**, 54–61.

FRANKENHAEUSER, B. AND HUXLEY, A. F. (1964). The action potential in the myelinated nerve of *Xenopus laevis* as computed on the basis of voltage clamp data. *J. Physiol., Lond.* **171**, 302–315.

HILLE, B. (1967). The selective inhibition of delayed potassium currents in nerve by tetraethylammonium ion. *J. gen. Physiol.*, **50**, 1287–1302.

HILLE, B. (1971). Voltage clamp studies on myelinated nerve fibres. In *Biophysics and Physiology of Excitable Membranes* (ed. W. J. Adelman), pp. 230–246. New York: Van Nostrand Reinhold.

HILLE, B. (1973). Potassium channels in myelinated nerve. Selective permeability to small cations. *J. gen Physiol.* **61**, 669–686.

HODGKIN, A. L. AND HUXLEY, A. F. (1952). A quantitative description of membrane current and its application to conduction and excitation in nerve. *J. Physiol., Lond.* **117**, 500–544.

NEUMCKE, B. (1981). Differences in electrophysiological properties of motor and sensory nerve fibres. *J. Physiol., Paris* **77**, 1135–1138.

NEUMCKE, B. AND STÄMPFLI, R. (1982). Sodium currents and sodium-current fluctuations in rat myelinated nerve fibres. *J. Physiol., Lond.* **329**, 163–184.

NONNER, W. (1969). A new voltage clamp method for Ranvier nodes. *Pflügers Arch. Eur. J. Physiol.* **309**, 176–192.

PLANT, T. D. (1986). The effects of rubidium ions on components of the potassium conductance in the frog node of Ranvier. *J. Physiol., Lond.* **375**, 81–105.

RACK, M. AND DREWS, G. (1989). Effects of a synthetic cationic polymer on sodium and potassium currents in frog nerve fibres. *Pflügers Arch. Eur. J. Physiol.* **413**, 610–615.

RÖPER, J. AND SCHWARZ, J. R. (1989). Heterogeneous distribution of fast and slow potassium channels in myelinated rat nerve fibres. *J. Physiol., Lond.* **416**, 93–110.

SCHWARZ, J. R., BROMM, B., SPIELMANN, R. P. AND WEYTJENS, J. L. F. (1983). Development of Na inactivation in motor and sensory myelinated nerve fibres of *Rana esculenta*. *Pflügers Arch. Eur. J. Physiol.* **398**, 126–129.

STÄMPFLI, R. AND HILLE, B. (1976). Electrophysiology of peripheral myelinated nerve. In *Frog Neurobiology* (ed. R. Llinas and W. Precht), pp. 3–32. Berlin: Springer-Verlag.